KU LEUVEN

6th International Symposium on Environmental Vibration (ISEV2013)
Tongji University, Shanghai, China, 8-10 November 2013

Mitigation of railway induced vibrations using stiff wave barriers

P. Coulier, S. François, G. Degrande and G. Lombaert

Department of Civil Engineering, KU Leuven, Belgium

Introduction

- EU FP7 project RIVAS "Railway Induced Vibration Abatement Solutions" (2011-2013).

- The project aims to reduce environmental vibration by providing a set of mitigation measures at the source, the track, the propagation path and the vehicle.
- 26 partners (railway operators, industry, consultancy, academics), coordination by UIC.
- www.rivas-project.eu
- **WP4 Mitigation measures on transmission/propagation.**
  - Trenches and buried wall barriers.
  - Subgrade stiffening.
  - Wave impeding blocks.
  - Masses along the surface (wave reflectors).

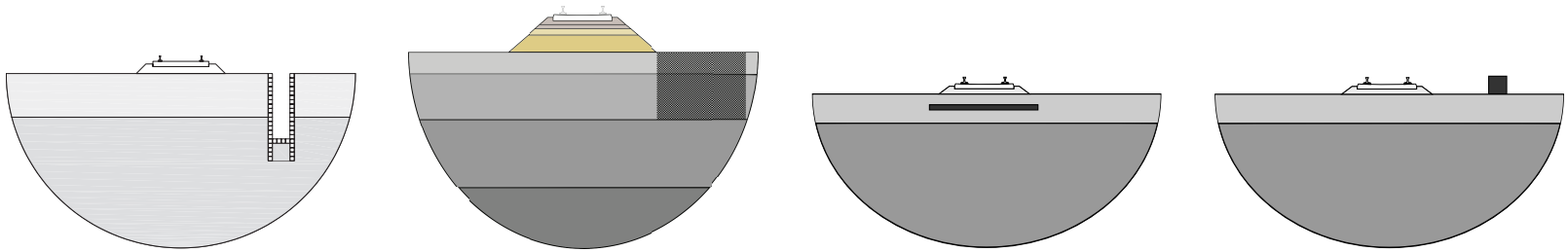

Stiff wave barrier next to the track

- Construction of a jet grouting wall next to the track.
- Wave impeding barrier for railway induced vibrations.

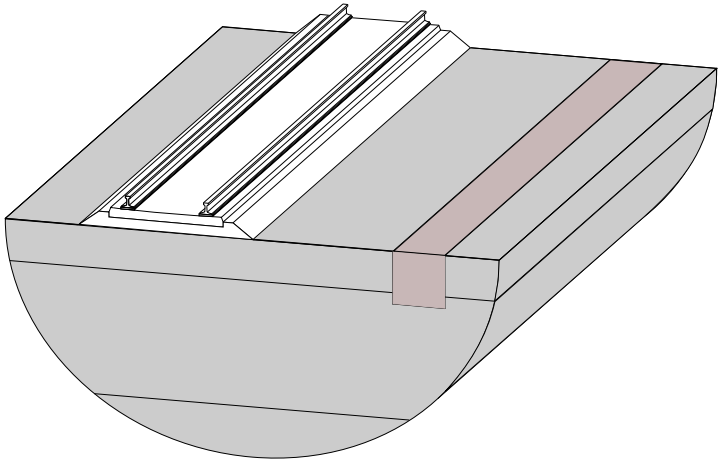

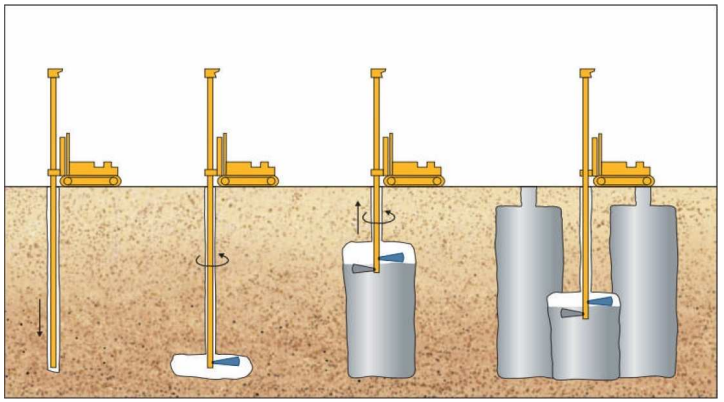

- Common construction techniques:
  - deep vibro compaction;
  - gravel/cement columns;
  - hydraulic fracture injection with stable cement–bentonite mixtures;
  - . . .

Stiff wave barrier

Problem outline

- Block of stiffened soil with square cross section (e.g. by means of jet grouting) embedded in a homogeneous halfspace next to a track on embankment [Coulier et al., SDEE, 2013].

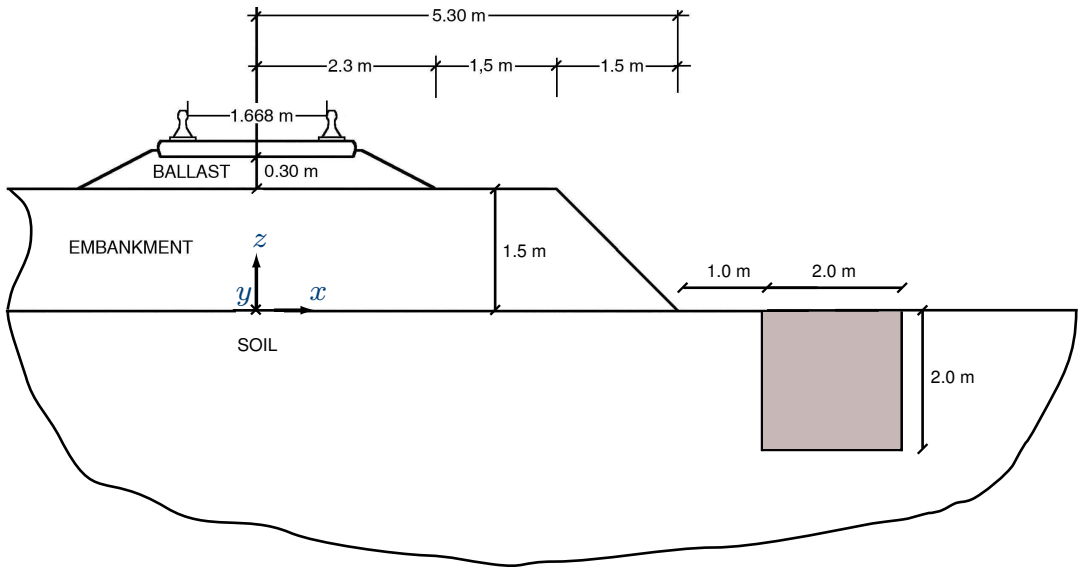

	C_s $[\mathrm{m/s}]$	C_p $[\mathrm{m/s}]$	β_s $[-]$	β_p $[-]$	ρ $[\mathrm{kg/m^3}]$
Halfspace	200	400	0.025	0.025	2000
Stiffened soil	550	950	0.050	0.050	2000

Transfer functions

- Real part of the vertical displacement $\hat{u}_z(\mathbf{x},\omega)$ at $5\,\mathrm{Hz}$:

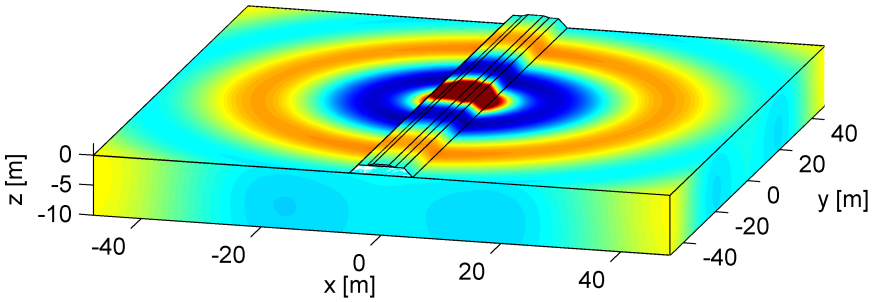

without barrier

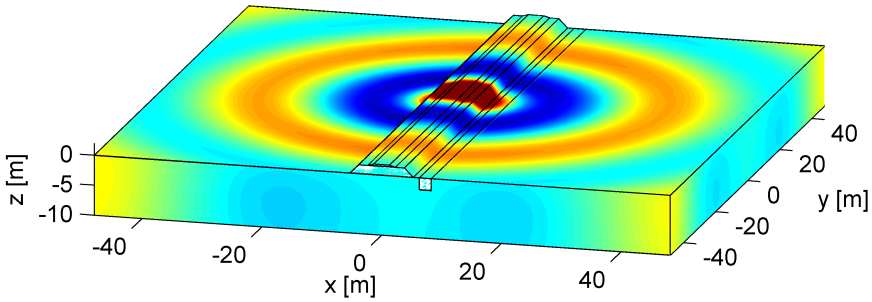

with barrier

- Corresponding insertion loss $\widehat{\mathrm{IL}}_z(\mathbf{x},\omega) = 20\log_{10}\frac{|\hat{u}_z^{\mathrm{ref}}(\mathbf{x},\omega)|}{|\hat{u}_z(\mathbf{x},\omega)|}$

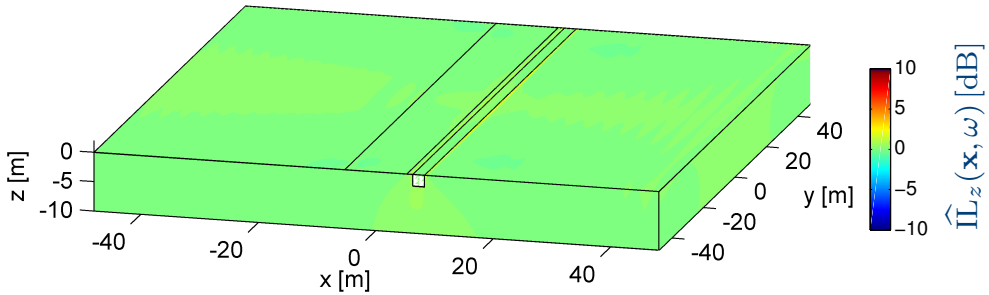

Transfer functions

- Real part of the vertical displacement $\hat{u}_z(\mathbf{x},\omega)$ at $30\,\mathrm{Hz}$:

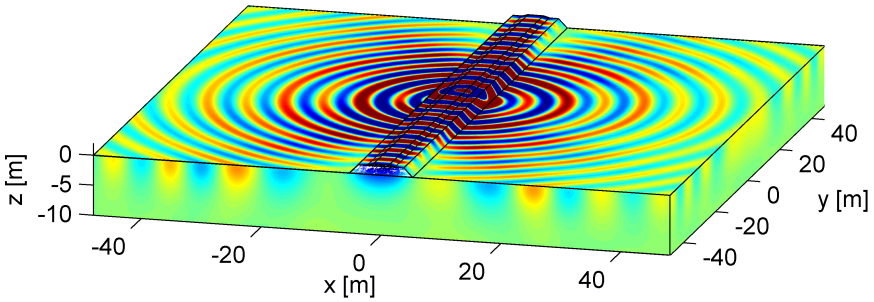

without barrier

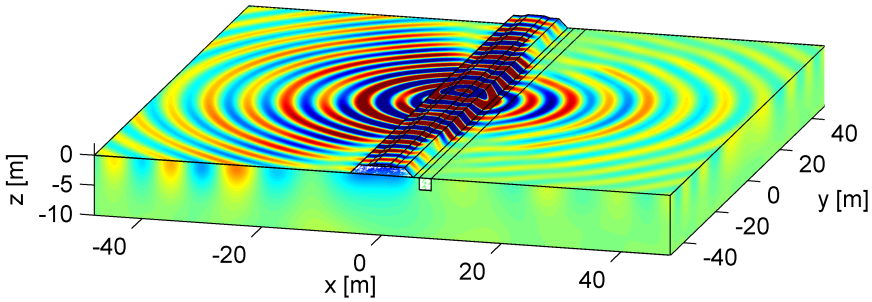

with barrier

- Corresponding insertion loss $\widehat{\mathrm{IL}}_z(\mathbf{x},\omega) = 20\log_{10}\frac{|\hat{u}_z^{\mathrm{ref}}(\mathbf{x},\omega)|}{|\hat{u}_z(\mathbf{x},\omega)|}$

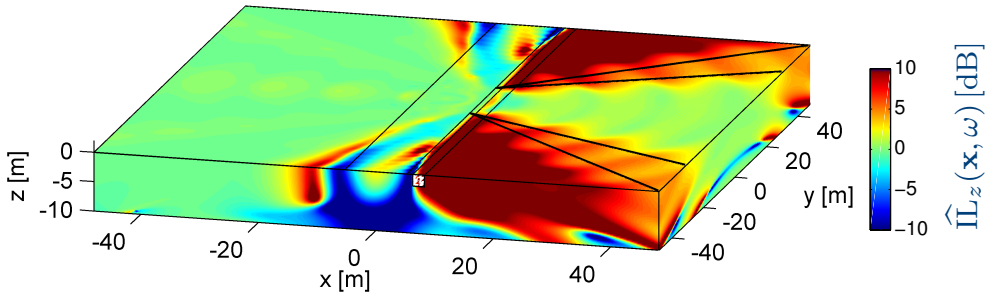

Transfer functions

- Real part of the vertical displacement $\hat{u}_z(\mathbf{x},\omega)$ at $60\,\mathrm{Hz}$:

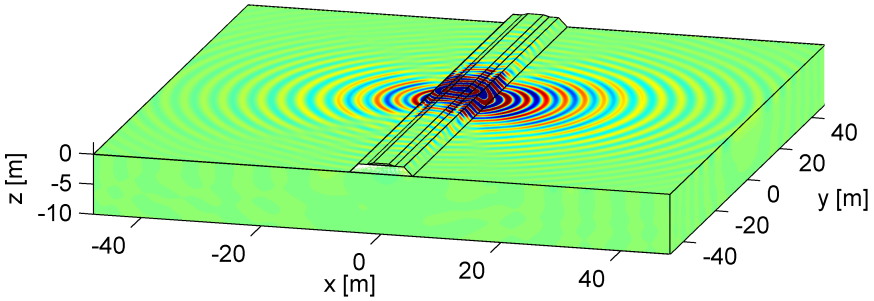

without barrier

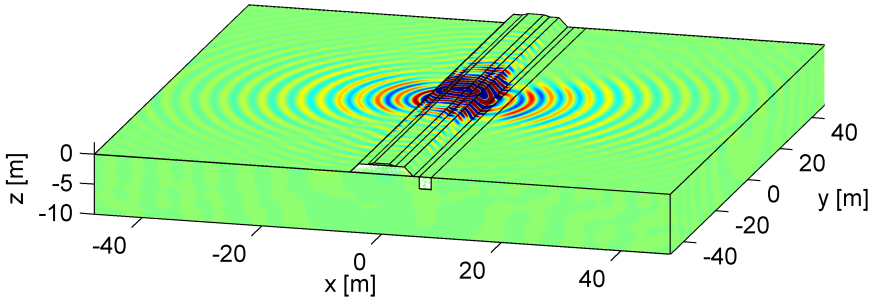

with barrier

- Corresponding insertion loss $\widehat{\mathrm{IL}}_z(\mathbf{x},\omega) = 20\log_{10}\frac{|\hat{u}_z^{\mathrm{ref}}(\mathbf{x},\omega)|}{|\hat{u}_z(\mathbf{x},\omega)|}$

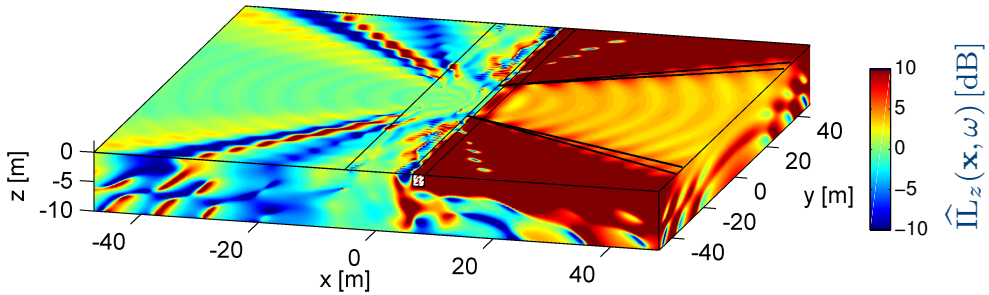

Plane wave propagation

- Cylindrical wavefield can be decomposed into plane waves, satisfying the dispersion relation $\frac{1}{\lambda_x^2} + \frac{1}{\lambda_y^2} = \frac{1}{\lambda_{\mathrm{R}}^2}$, where $\lambda_{\mathrm{R}} = 2\pi \frac{C_{\mathrm{R}}}{\omega}$ is the Rayleigh wavelength.

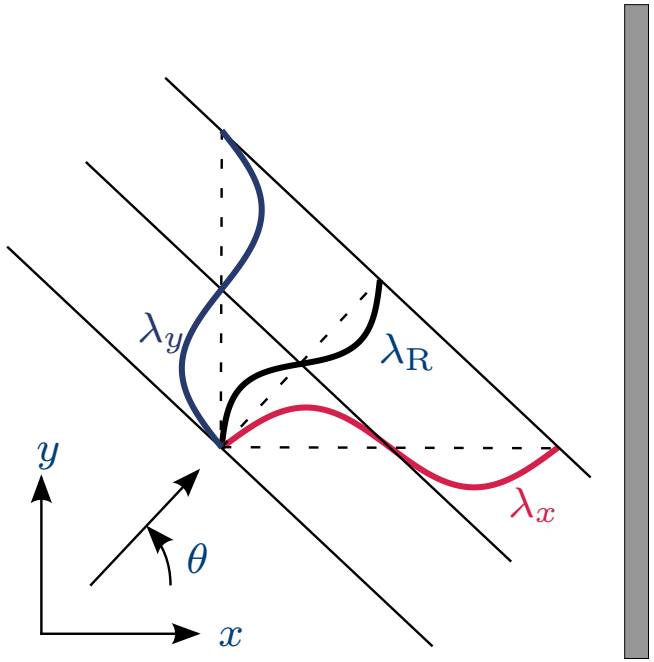

- Propagating plane waves are characterized by $\lambda_{\mathrm{R}} \leqslant \lambda_y \leqslant \infty$:
  - $\theta = 0 \Rightarrow \lambda_x = \lambda_{\mathrm{R}}, \lambda_y = \infty$
  - $\theta = \pi/2 \Rightarrow \lambda_x = \infty, \lambda_y = \lambda_{\mathrm{R}}$

Stiff wave barrier

Plane wave propagation

- Plane wave propagation (a) without and (b) with stiff wave barrier for $\lambda_y = \infty$ ($\theta = 0$).

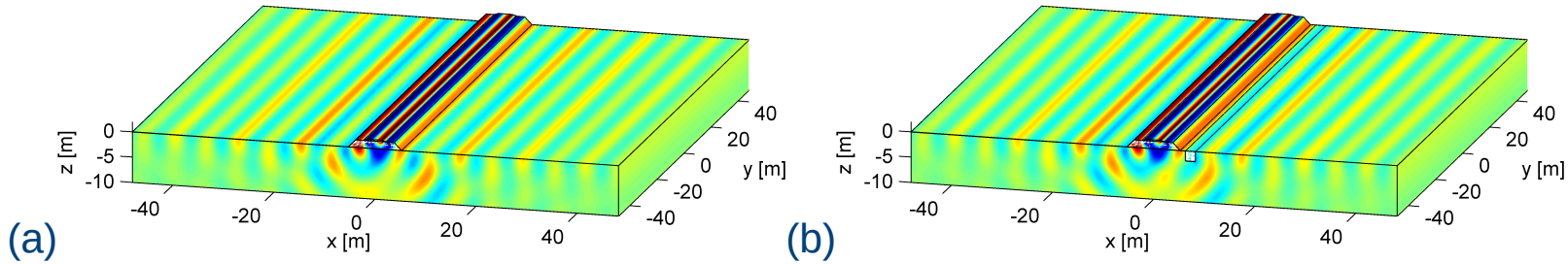

- Plane wave propagation (a) without and (b) with stiff wave barrier for $\lambda_{\mathrm{R}} \leqslant \lambda_y \leqslant \infty$ ($\theta = 0.50$).

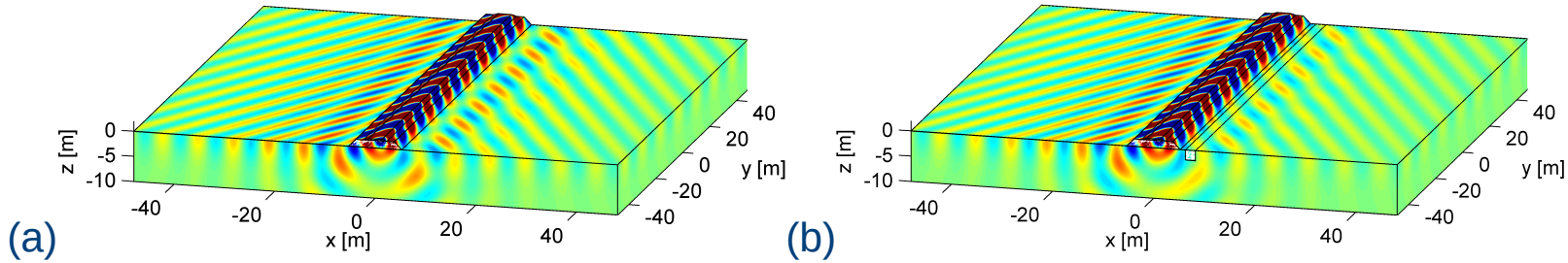

Plane wave propagation

- Plane wave propagation (a) without and (b) with stiff wave barrier for $\lambda_{\mathrm{R}} \leqslant \lambda_y \leqslant \infty$ ($\theta = 1.2$).

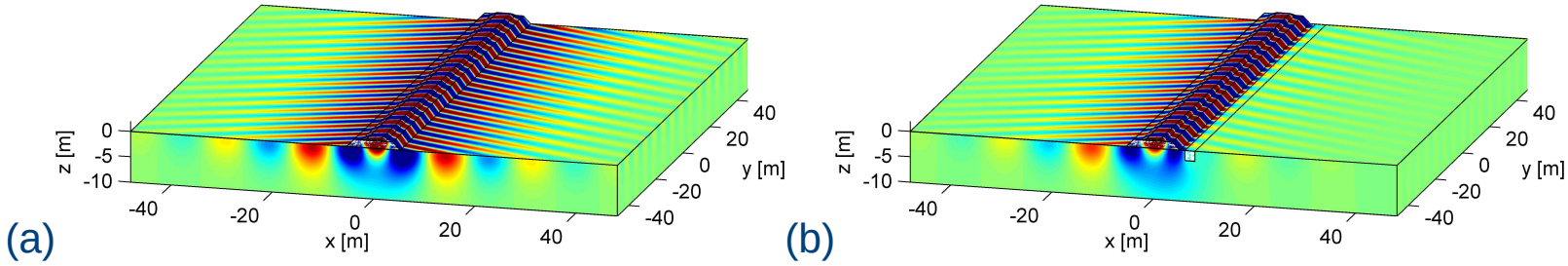

- Plane wave propagation (a) without and (b) with stiff wave barrier for $\lambda_y < \lambda_{\mathrm{R}}$ ($\theta = \pi/2$).

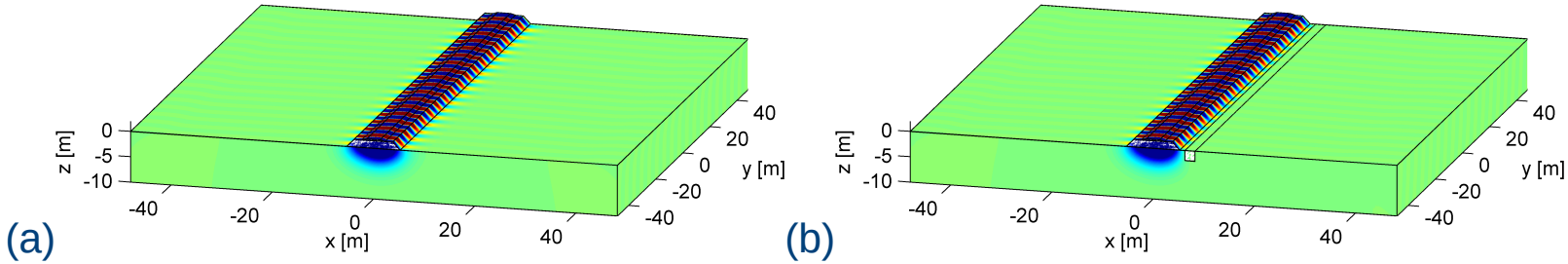

Stiff wave barrier

Interaction of Rayleigh waves in the soil and bending waves in the stiff wave barrier

- Rayleigh wave dispersion curve (black line):

$$\lambda_{\mathrm{R}} = 2\pi \frac{C_{\mathrm{R}}}{\omega}$$

- Euler-Bernoulli beam theory in (λ_y, ω)-domain:

$$\left(-\rho A \omega^2 + EI \left(\frac{2\pi}{\lambda_y} \right)^4 \right) \tilde{u}_z(\lambda_y, \omega) = \tilde{f}(\lambda_y, \omega)$$

- Free bending wave dispersion curve (red line):

$$\lambda_{\mathrm{b}} = \frac{2\pi}{\sqrt{\omega}} \left(\frac{EI}{\rho A} \right)^{1/4}$$

$$\Rightarrow \tilde{u}_z(\lambda_y, \omega) \propto 0 \text{ for } \lambda_y < \lambda_{\mathrm{b}}$$

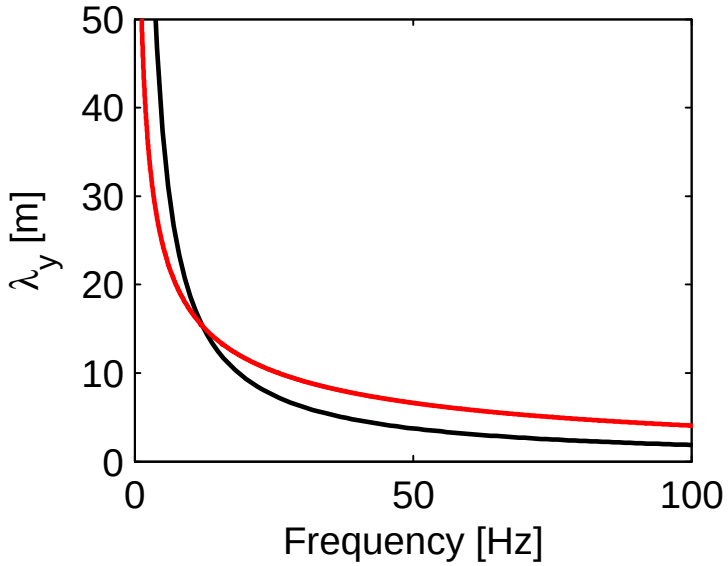

$\lambda_y = \infty$

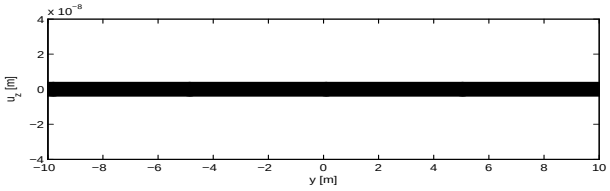

$\lambda_y = \lambda_{\mathrm{b}}$

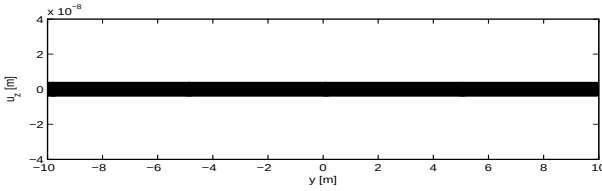

$\lambda_y = 2/3\lambda_{\mathrm{b}}$

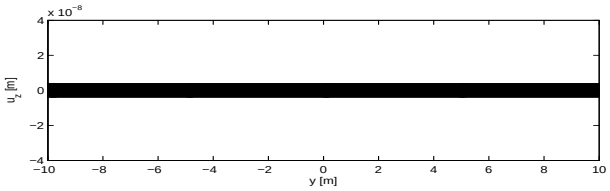

$\lambda_y = 1/3\lambda_{\mathrm{b}}$

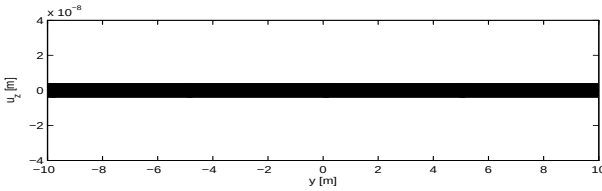

Stiff wave barrier

Interaction of Rayleigh waves in the soil and bending waves in the stiff wave barrier

- $f < f_\mathrm{c}$: $\lambda_\mathrm{R} > \lambda_\mathrm{b} \Rightarrow$ Rayleigh wave propagates unhindered through the block of stiffened soil
- $f > f_\mathrm{c}$: $\lambda_\mathrm{R} < \lambda_\mathrm{b} \Rightarrow$ wave field is partially transmitted, partially blocked
  - $\lambda_y > \lambda_\mathrm{b}$: plane waves are transmitted ($\widehat{\mathrm{IL}}_z(\mathbf{x},\omega) \sim 0\,\mathrm{dB}$)
  - $\lambda_y < \lambda_\mathrm{b}$: transmission of plane waves is impeded by the block of stiffened soil

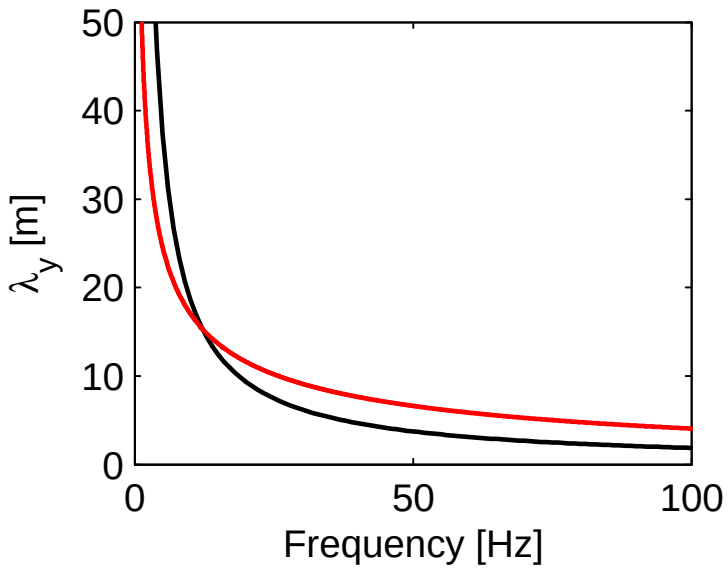

- Critical frequency f_c (intersection of the Rayleigh wave and the free bending wave dispersion curves):

$$f_\mathrm{c} = \frac{\omega_\mathrm{c}}{2\pi} = \frac{C_\mathrm{R}^2}{2\pi}\sqrt{\frac{\rho A}{EI}} = \frac{C_\mathrm{R}^2}{2\pi h}\sqrt{\frac{12\rho}{E}} = 12\,\mathrm{Hz}$$

Interaction of Rayleigh waves in the soil and bending waves in the stiff wave barrier

- The propagating plane waves $\lambda_y > \lambda_\mathrm{R}$ are characterized by a wave propagation direction $\theta = \sin^{-1}(\lambda_\mathrm{R}/\lambda_y)$.
  A reduction of vibration levels in the spatial domain will only be obtained in an area delimited by a critical angle $\theta_\mathrm{c}(\omega) = \sin^{-1}(\lambda_\mathrm{R}/\lambda_\mathrm{b})$:

$$\sin\theta_\mathrm{c} = \frac{C_\mathrm{R}}{\sqrt{\omega}}\left(\frac{\rho A}{EI}\right)^{1/4} = \frac{C_\mathrm{R}}{\sqrt{\omega h}}\left(\frac{12\rho}{E}\right)^{1/4}$$

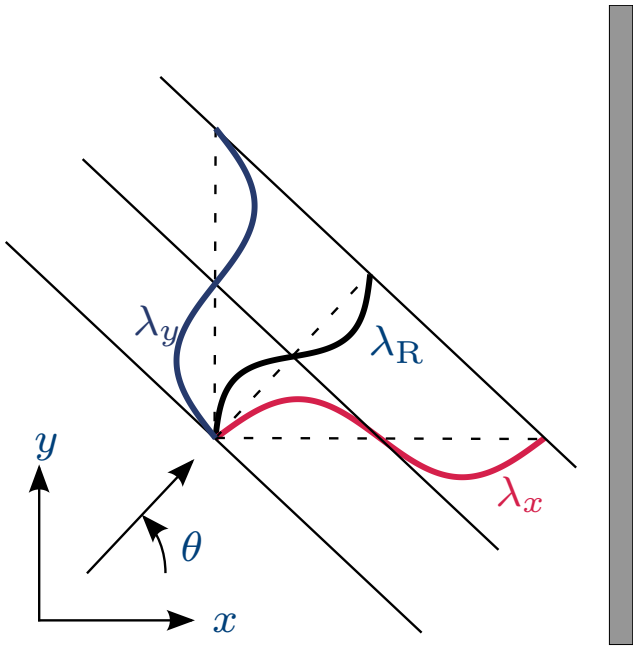

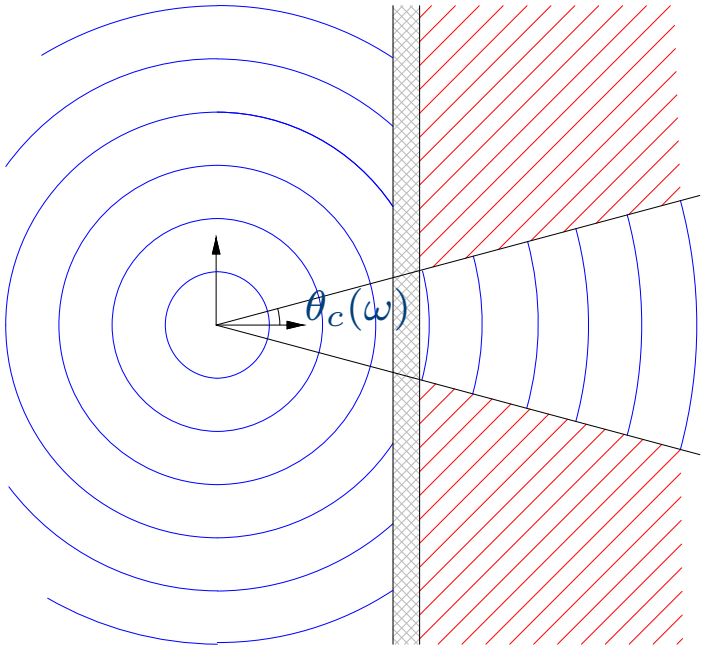

Passage of a Renfe S599 train

- Renfe S599 train composition.

	N_a [−]	L_t [m]	L_b [m]	L_a [m]	M_u [kg]
Two motor coaches	4	25.85	17.73	2.50	1940
One central carriage	4	24.28	18.00	2.50	1704

- Simplified vehicle model: only the unsprung masses are taken into account
- Hertzian contact spring: $k_\mathrm{Hz} = 3 \times 10^9\,\mathrm{N/m}$.
- Track unevenness: FRA class 3.
- Train speed: $v = 160\,\mathrm{km/h}$.

Passage of a Renfe S599 train

- One–third octave band RMS spectra of the vertical free field vibrations in the reference case (black lines) and in case of stiffening next to the track (grey lines) for the passage of a Renfe S599 train at a speed of $160\,\mathrm{km/h}$.

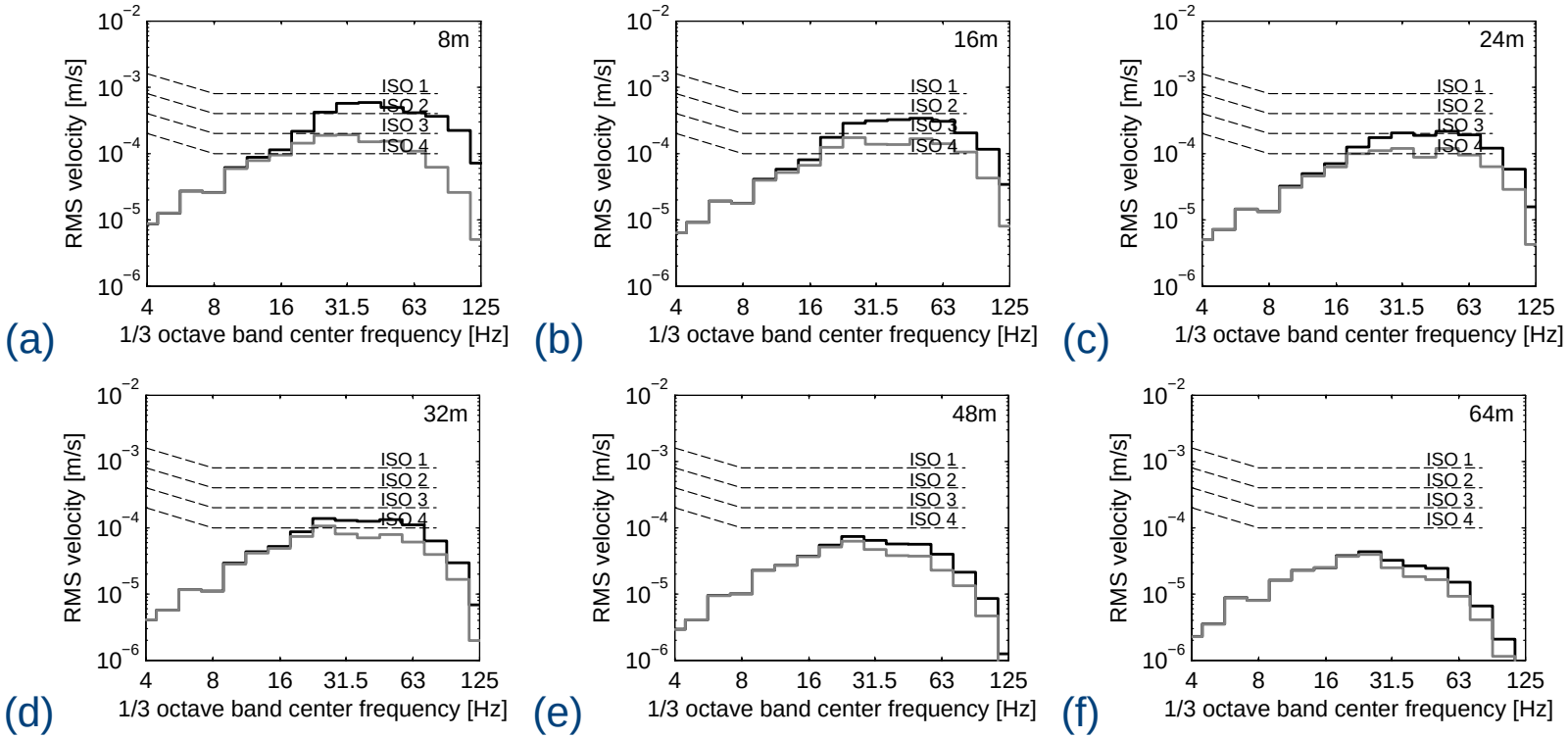

- In case of subgrade stiffening next to the track, a reduction of vibration levels can only be obtained from the critical frequency of $12\,\mathrm{Hz}$ on.

Stiff wave barrier

Insertion loss

- Vertical insertion loss $\widehat{\mathrm{IL}}_z(\mathbf{x},\omega)$ at $8\,\mathrm{m}$, $16\,\mathrm{m}$, $24\,\mathrm{m}$, $32\,\mathrm{m}$, $48\,\mathrm{m}$ and $64\,\mathrm{m}$ from the center of the track (black to light grey lines) due to the passage of a Renfe S599 train at a speed of $160\,\mathrm{km/h}$.

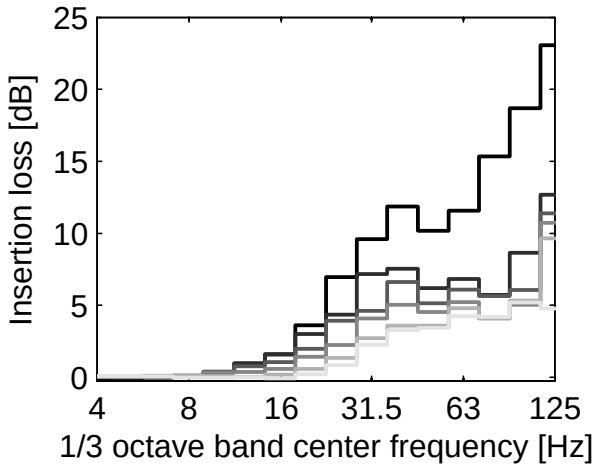

  - $\widehat{\mathrm{IL}}_z(x_1,\bar{\omega}) > \widehat{\mathrm{IL}}_z(x_2,\bar{\omega})$ for $x_1 < x_2$
  - $\widehat{\mathrm{IL}}_z(\bar{x},\omega_1) < \widehat{\mathrm{IL}}_z(\bar{x},\omega_2)$ for $\omega_1 < \omega_2$

- $\omega_1 > \omega_c$:
  - $\mathbf{x}_1$: axle loads $\hat{\mathbf{g}}_{i-1}(\omega)$ to $\hat{\mathbf{g}}_{i+1}(\omega)$
  - $\mathbf{x}_2$: axle loads $\hat{\mathbf{g}}_{i-3}(\omega)$ to $\hat{\mathbf{g}}_{i+3}(\omega)$

- ω_2 ($\omega_c < \omega_1 < \omega_2$):
  - $\mathbf{x}_1$: axle load $\hat{\mathbf{g}}_i(\omega)$
  - $\mathbf{x}_2$: axle loads $\hat{\mathbf{g}}_{i-1}(\omega)$ to $\hat{\mathbf{g}}_{i+1}(\omega)$

- $\omega_2 > \omega_1$: $\theta_c(\omega_2) < \theta_c(\omega_1) \Rightarrow$ the area in which the transfer to the free field is impeded, is enlarged

Physical interpretation for moving axle loads

- Top view of the track, the block of stiffened soil next to the track and the free field. Superimposed are lines indicating the critical angle $\theta_c(\omega)$ at a frequency (a) ω_1 and (b) ω_2, with $\omega_c < \omega_1 < \omega_2$.

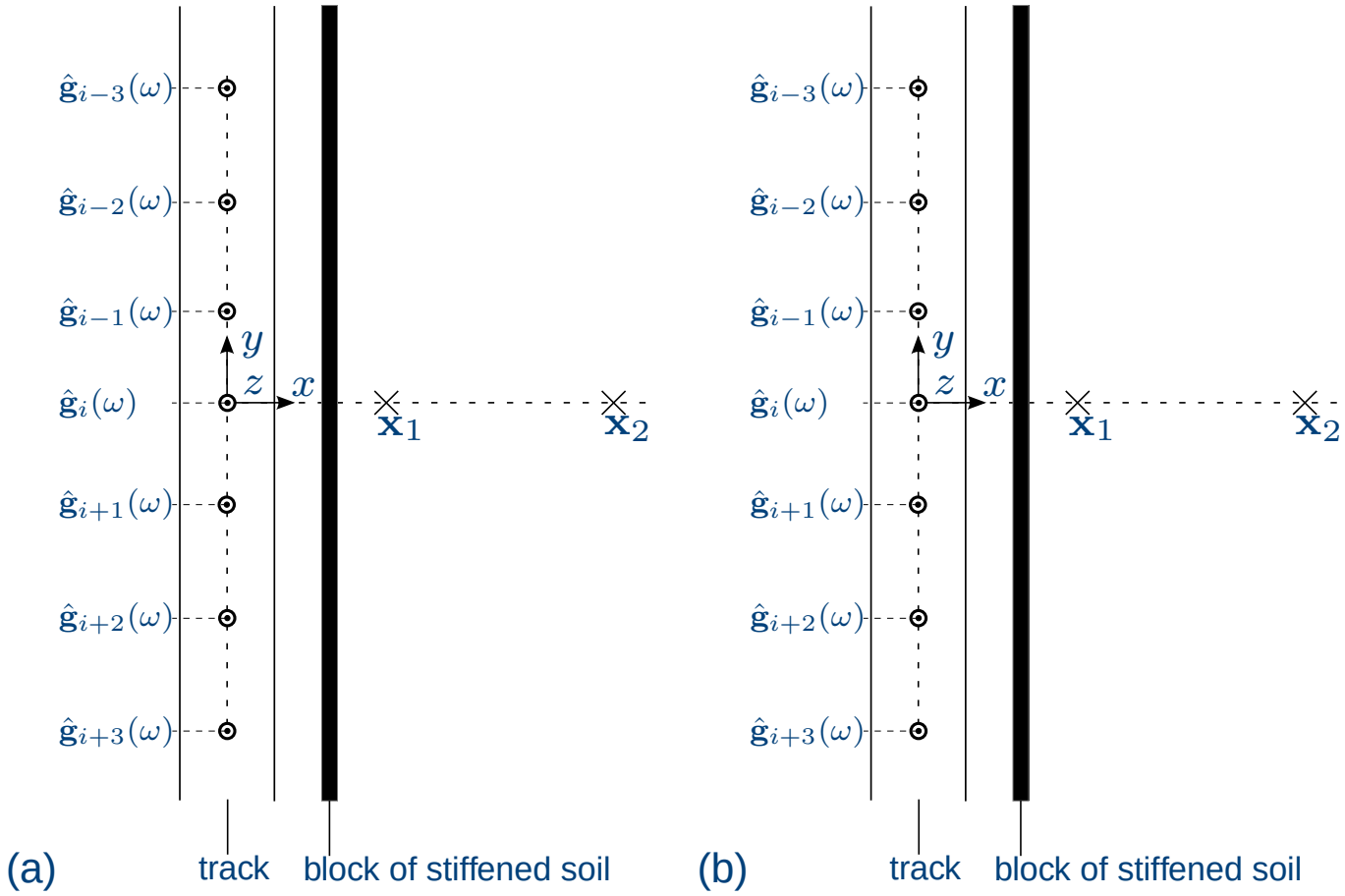

Physical interpretation for moving axle loads

- Top view of the track, the block of stiffened soil next to the track and the free field. Superimposed are lines indicating the critical angle $\theta_c(\omega)$ at a frequency (a) ω_1 and (b) ω_2, with $\omega_c < \omega_1 < \omega_2$.

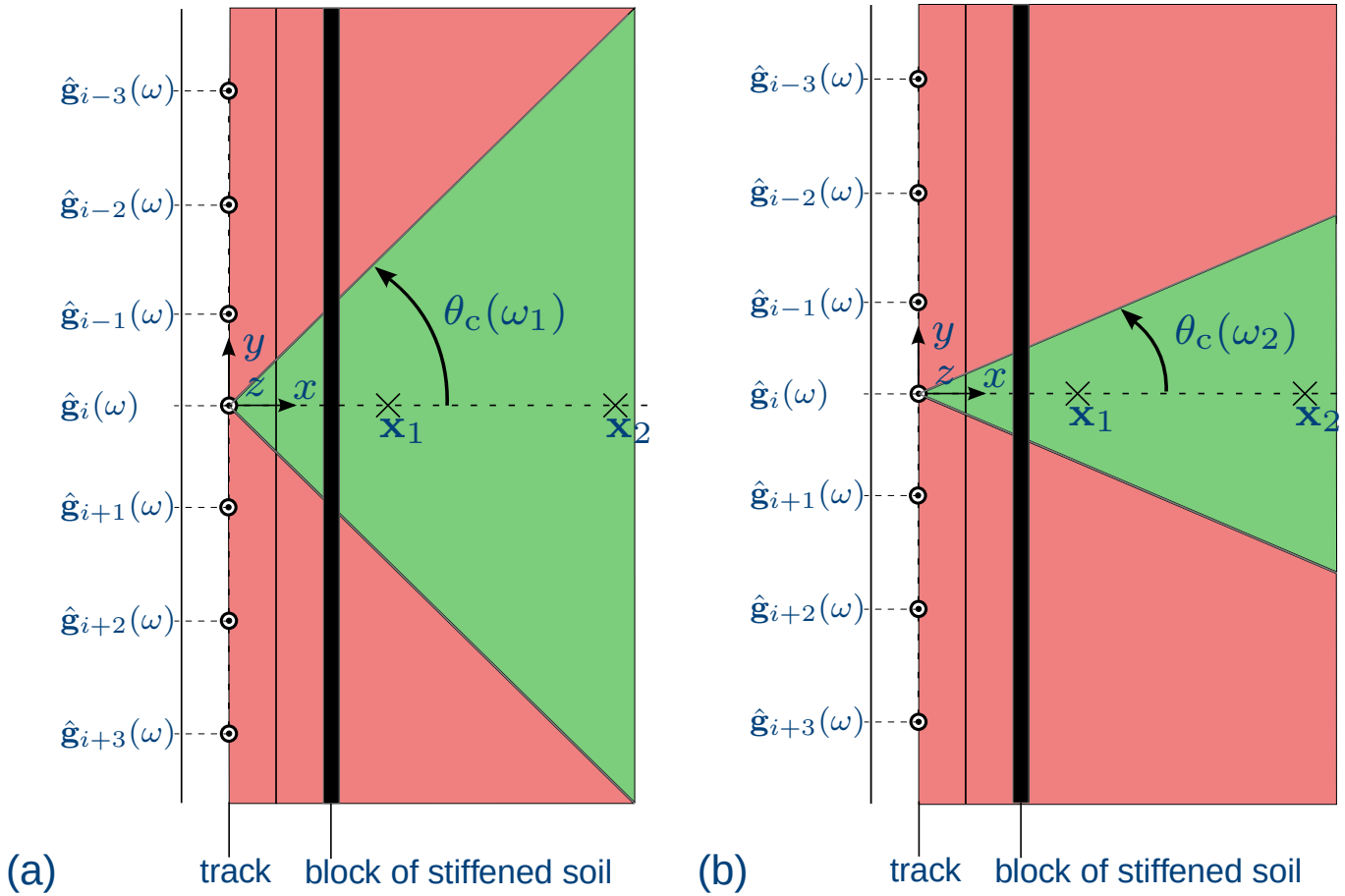

Physical interpretation for moving axle loads

- Top view of the track, the block of stiffened soil next to the track and the free field. Superimposed are lines indicating the critical angle $\theta_c(\omega)$ at a frequency (a) ω_1 and (b) ω_2, with $\omega_c < \omega_1 < \omega_2$.

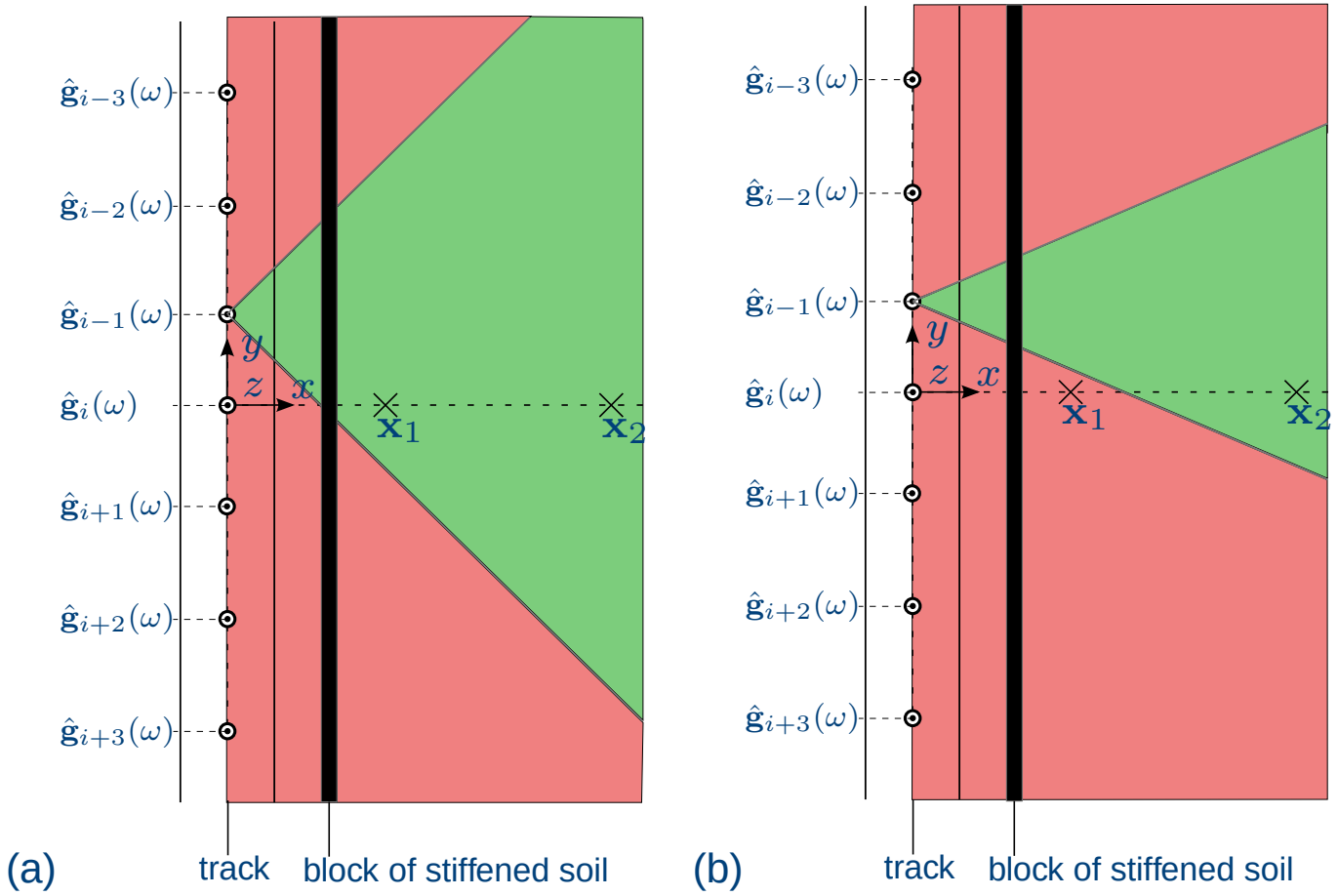

Physical interpretation for moving axle loads

- Top view of the track, the block of stiffened soil next to the track and the free field. Superimposed are lines indicating the critical angle $\theta_c(\omega)$ at a frequency (a) ω_1 and (b) ω_2, with $\omega_c < \omega_1 < \omega_2$.

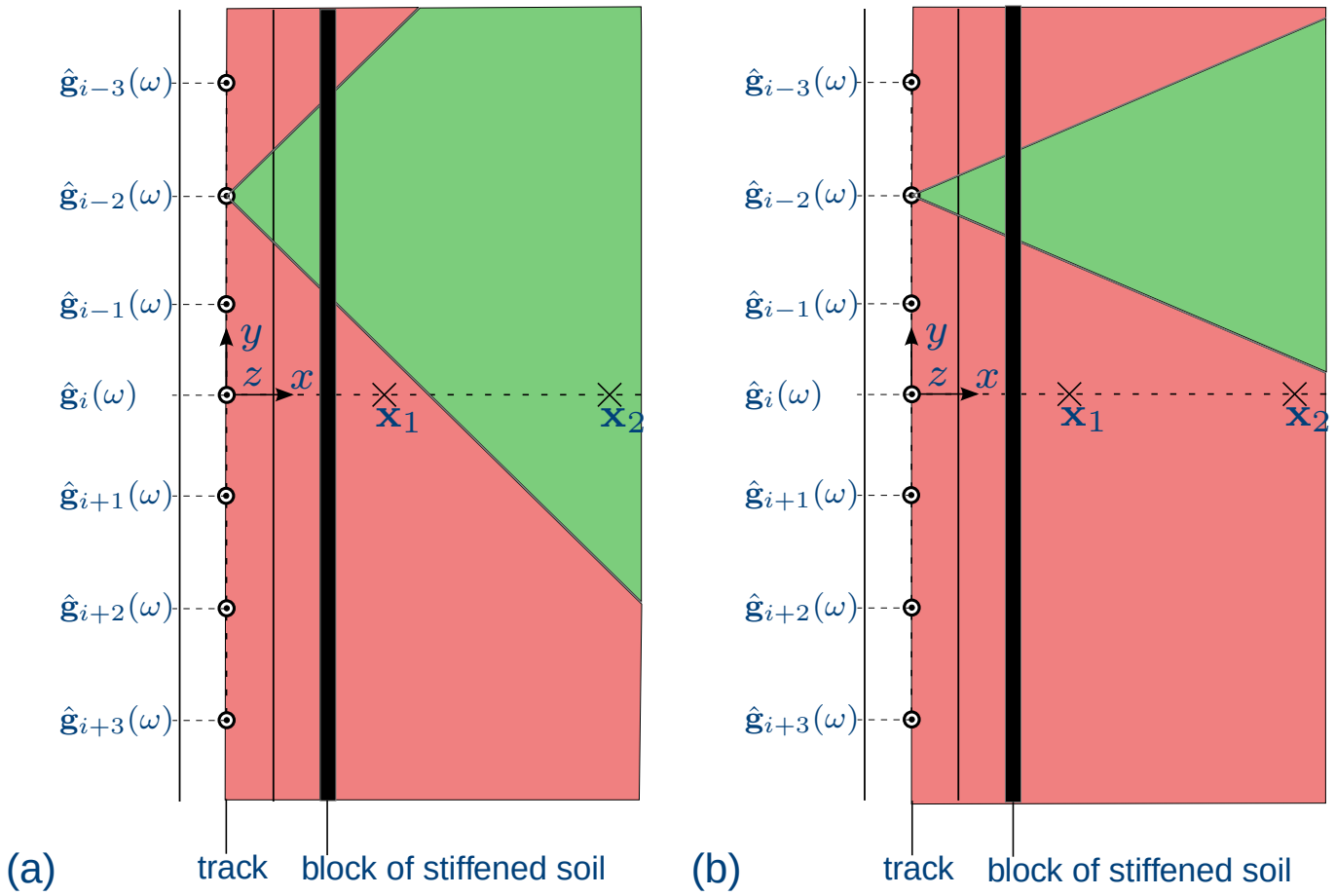

Physical interpretation for moving axle loads

- Top view of the track, the block of stiffened soil next to the track and the free field. Superimposed are lines indicating the critical angle $\theta_c(\omega)$ at a frequency (a) ω_1 and (b) ω_2, with $\omega_c < \omega_1 < \omega_2$.

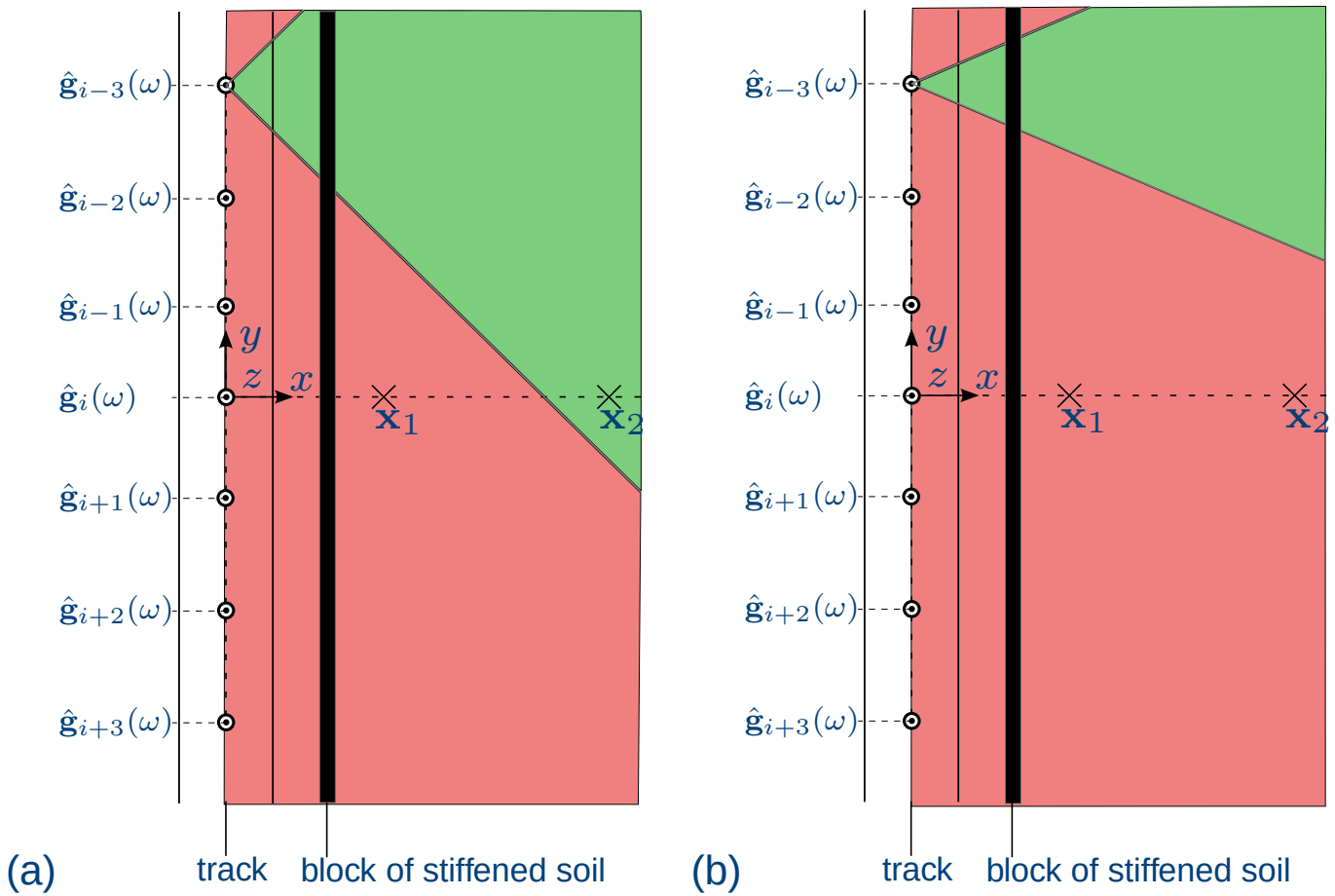

Transfer functions for a stiff wave barrier with finite length

- Real part of the vertical displacement $\hat{u}_z(\mathbf{x}, \omega)$ at $60\,\mathrm{Hz}$ for a block of stiffened soil with a length of (a) $15\,\mathrm{m}$, (b) $30\,\mathrm{m}$, (c) $45\,\mathrm{m}$, (d) $60\,\mathrm{m}$, and (e) ∞.

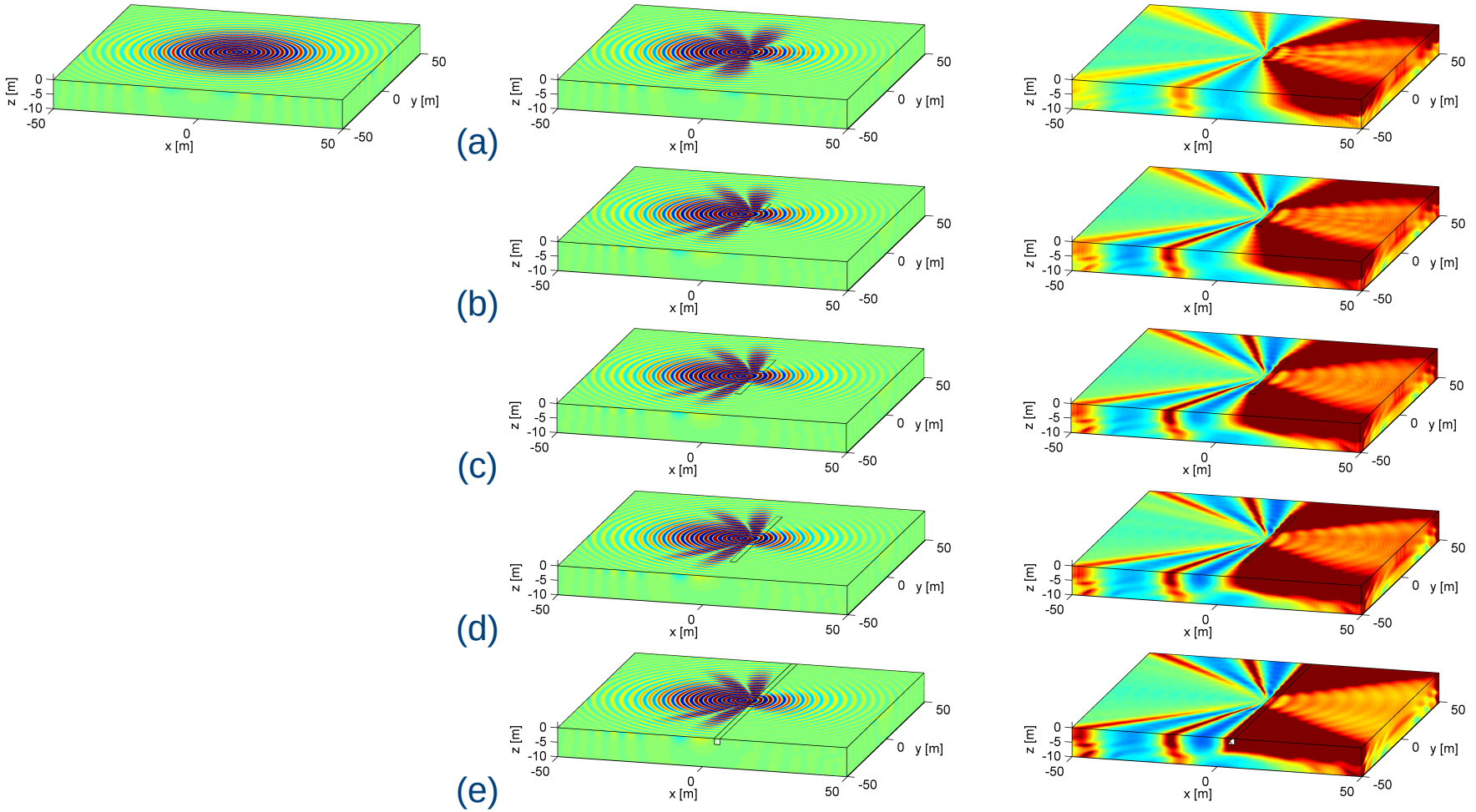

without barrier | with barrier | insertion loss $\widehat{\mathrm{IL}}_z(\mathbf{x}, \omega)$

El Realengo test site

Test and reference site

- Conventional railway line (ADIF) between Murcia and Alicante.
- Low Segura river flood plain.

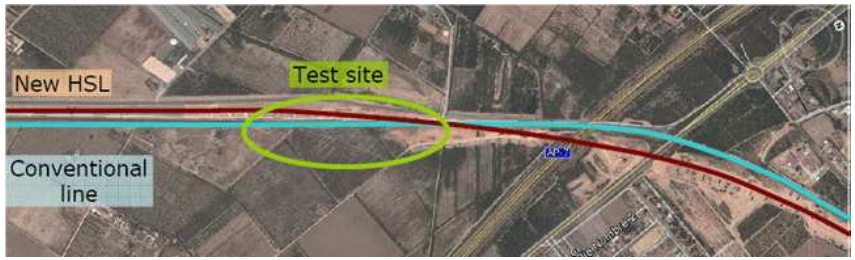

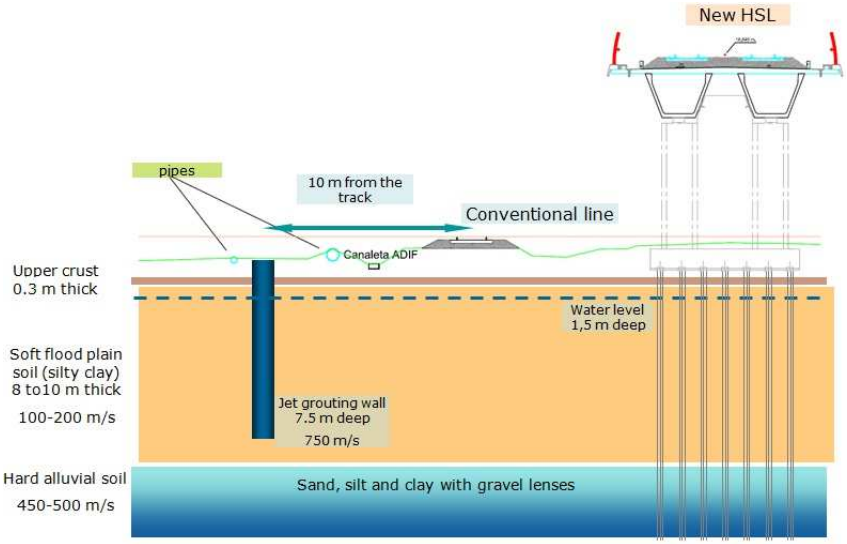

- (a) S592 commuter train, (b) S599 medium distance train and (c) Talgo VI train.

(a) 

(b) 

(c) 

- Construction of a new HST line between Madrid and Levante.
- Installation of a jet grouting wall next to track as a vibration mitigation measure.

Dynamic soil characteristics

Shear wave velocity

- Spectral Analysis of Surface Waves (falling weight deflectometer, CEDEX).
- Seismic Cone Penetration Test (down-hole test, CEDEX).

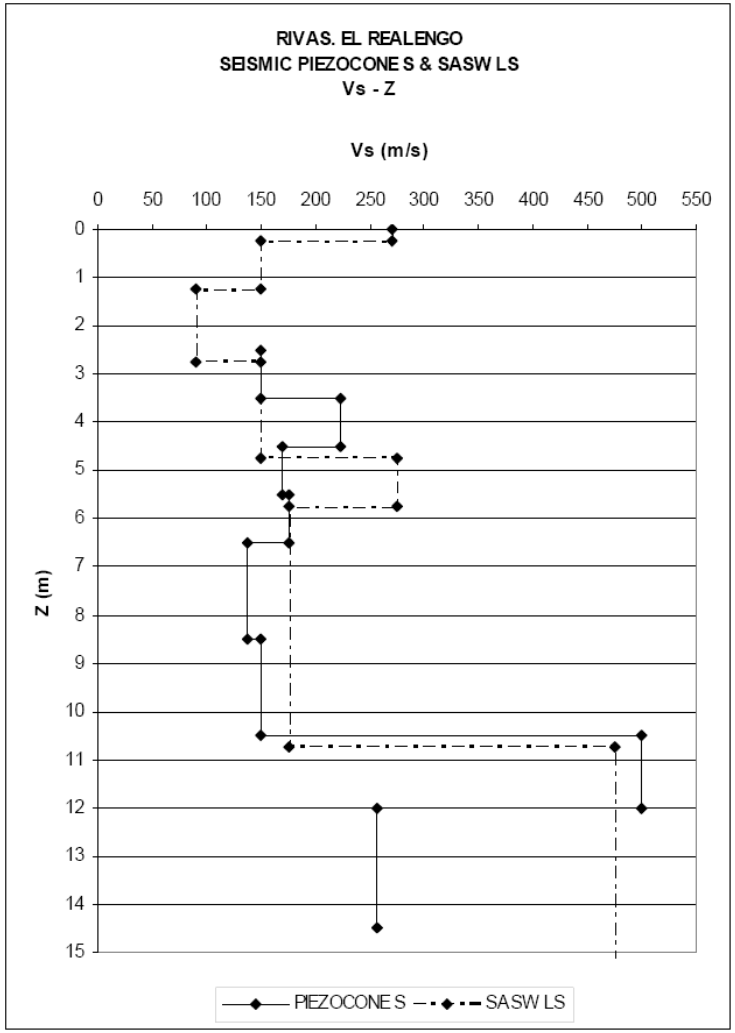

Dynamic soil characteristics

Longitudinal wave velocity

- Seismic refraction test (CEDEX).

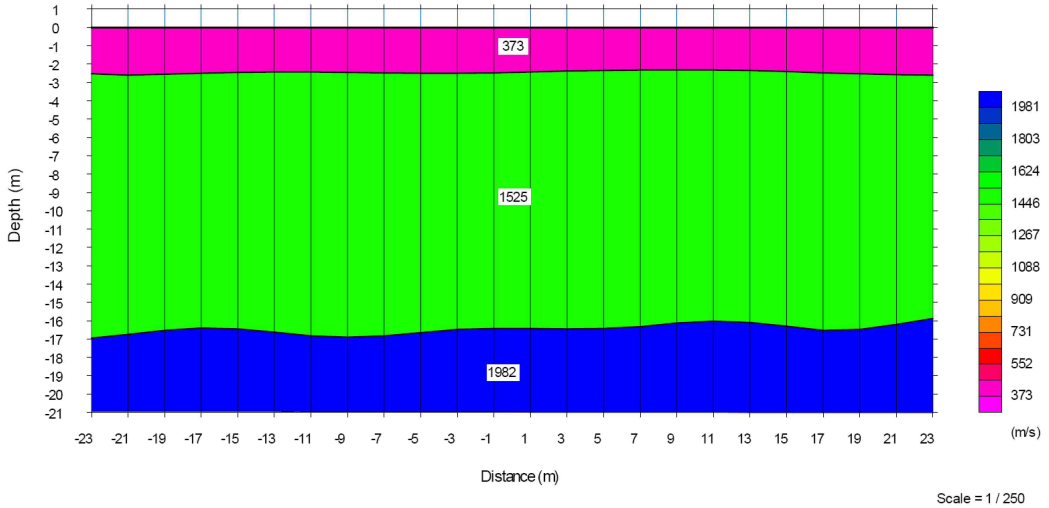

Identified soil profile

Layer	h [m]	C_s [m/s]	C_p [m/s]	β_s [−]	β_p [−]	ρ [kg/m^3]
1	0.30	270	560	0.025	0.025	1800
2	1.20	150	470	0.025	0.025	1750
3	8.50	150	1560	0.025	0.025	1750
4	10.00	475	1560	0.025	0.025	1900
5	∞	550	2030	0.025	0.025	1900

Dynamic soil characteristics

Material damping ratio

- Measured Arias intensity at the test (red line) and reference (green line) section and predicted Arias intensity (a) before and (b) after updating of the material damping ratio [Badsar, 2012].

$$I_{zz}^{\mathrm{E}}(r) = \frac{\pi}{2g}\int_{-\infty}^{+\infty} a^2(r,t)\mathrm{d}t \qquad (1)$$

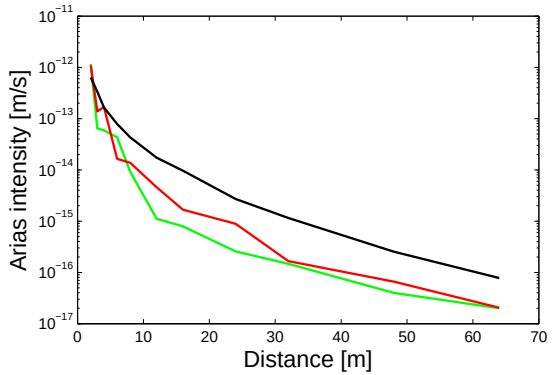

(a)

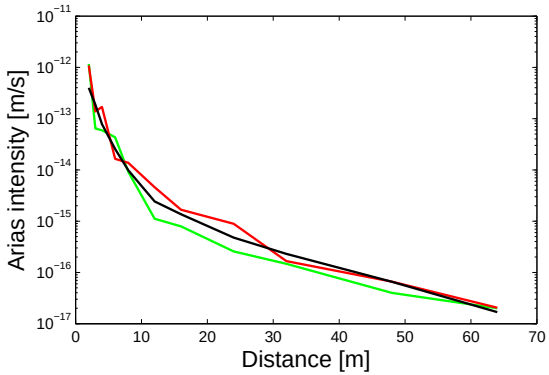

(b)

Identified soil profile (update)

Layer	h [m]	C_{s} [m/s]	C_{p} [m/s]	β_{s} [−]	β_{p} [−]	ρ [kg/m^3]
1	0.30	270	560	0.123	0.123	1800
2	1.20	150	470	0.112	0.112	1750
3	8.50	150	1560	0.014	0.014	1750
4	10.00	475	1560	0.010	0.010	1900
5	∞	550	2030	0.010	0.010	1900

Track characteristics

- RN 45 rails:
  $EI_{\mathrm{r}} = 3.00 \times 10^6$ Nm^2 and $\rho A_{\mathrm{r}} = 44.8$ kg/m.
- Bi-block reinforced concrete sleepers:
  $m_{\mathrm{sl}} = 200$ kg and spacing $d = 0.6$ m.
- Rubber rail pads with a thickness of 4.5 mm and stiffness of 300 kN/mm.
- Ballast layer ($d = 0.50$ m, $C_{\mathrm{s}} = 250$ m/s, $\nu = 0.2$ and $\rho = 1600$ kg/m^3).
- Embankment ($d = 0.50$ m, $C_{\mathrm{s}} = 200$ m/s, $\nu = 0.35$ and $\rho = 1700$ kg/m^3).

Numerical simulations

Jet grouting wall dimensions

- Variant A: $w = 1\,\mathrm{m}$, $h = 5\,\mathrm{m}$

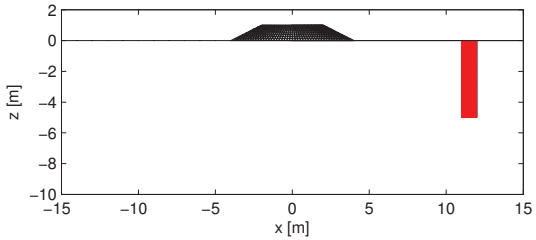

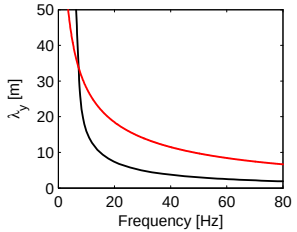

- Variant B: $w = 1\,\mathrm{m}$, $h = 7.5\,\mathrm{m}$

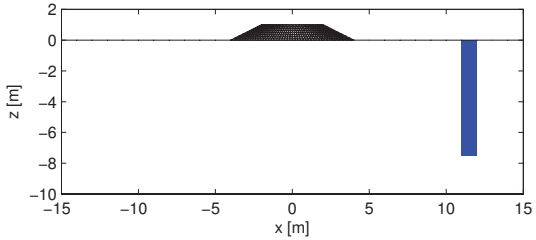

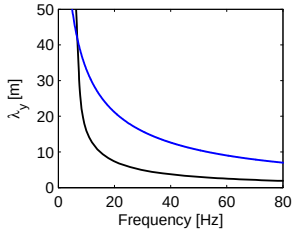

- Variant C: $w = 1\,\mathrm{m}$, $h = 10\,\mathrm{m}$

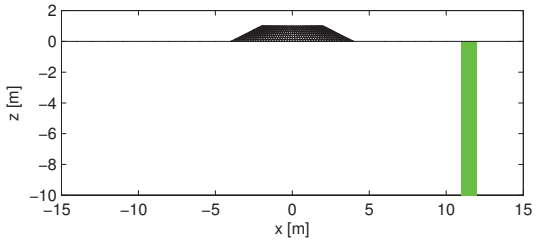

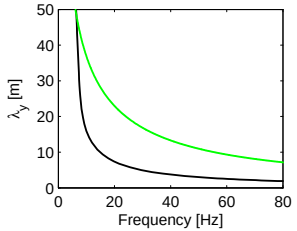

C_s [m/s]	C_p [m/s]	β_s [−]	β_p [−]	ρ [kg/m^3]
650	1125	0.030	0.030	2200

Transfer functions (variant A)

- Real part of the vertical displacement $\hat{u}_z(\mathbf{x}, \omega)$ at (a) $5\,\mathrm{Hz}$, (b) $30\,\mathrm{Hz}$ and (c) $60\,\mathrm{Hz}$ without (left) and with (middle) barrier and insertion loss (right)

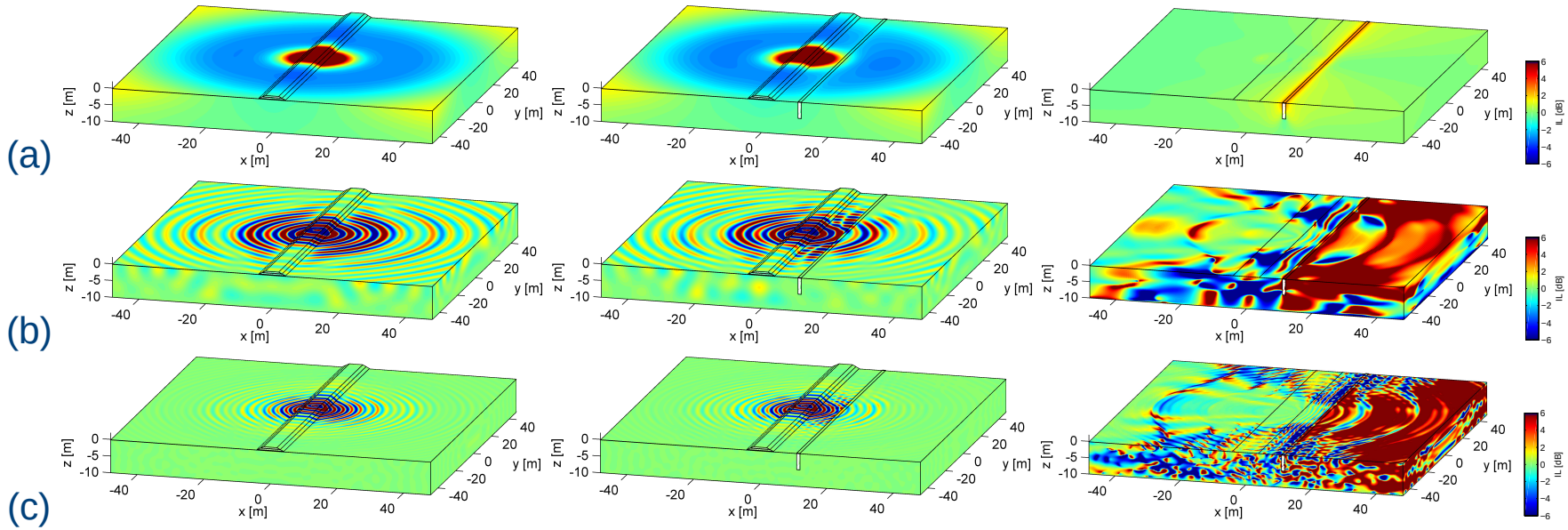

Passage of a S592 commuter train

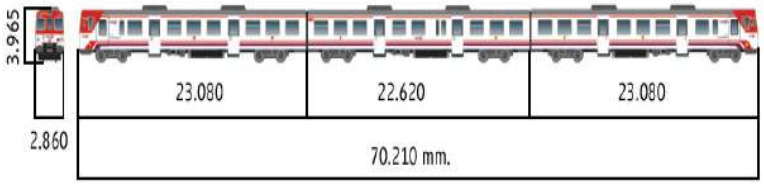

- Simplified vehicle model: only the unsprung masses are taken into account ($M_{\mathrm{u}} = 2000\,\mathrm{kg}$)
- Hertzian contact spring: $k_{\mathrm{Hz}} = 3 \times 10^9\,\mathrm{N/m}$.
- Track unevenness: FRA class 3.
- Train speed: $v = 120\,\mathrm{km/h}$.

Passage of a S592 commuter train

- One–third octave band vertical insertion loss $\widehat{\mathrm{IL}}_z(\mathbf{x}, \omega)$ at (a) $8\,\mathrm{m}$, (b) $16\,\mathrm{m}$, (c) $24\,\mathrm{m}$, (d) $32\,\mathrm{m}$, (e) $48\,\mathrm{m}$ and (f) $64\,\mathrm{m}$ from the center of the track for the passage of a S592 commuter train at a speed of $120\,\mathrm{km/h}$.

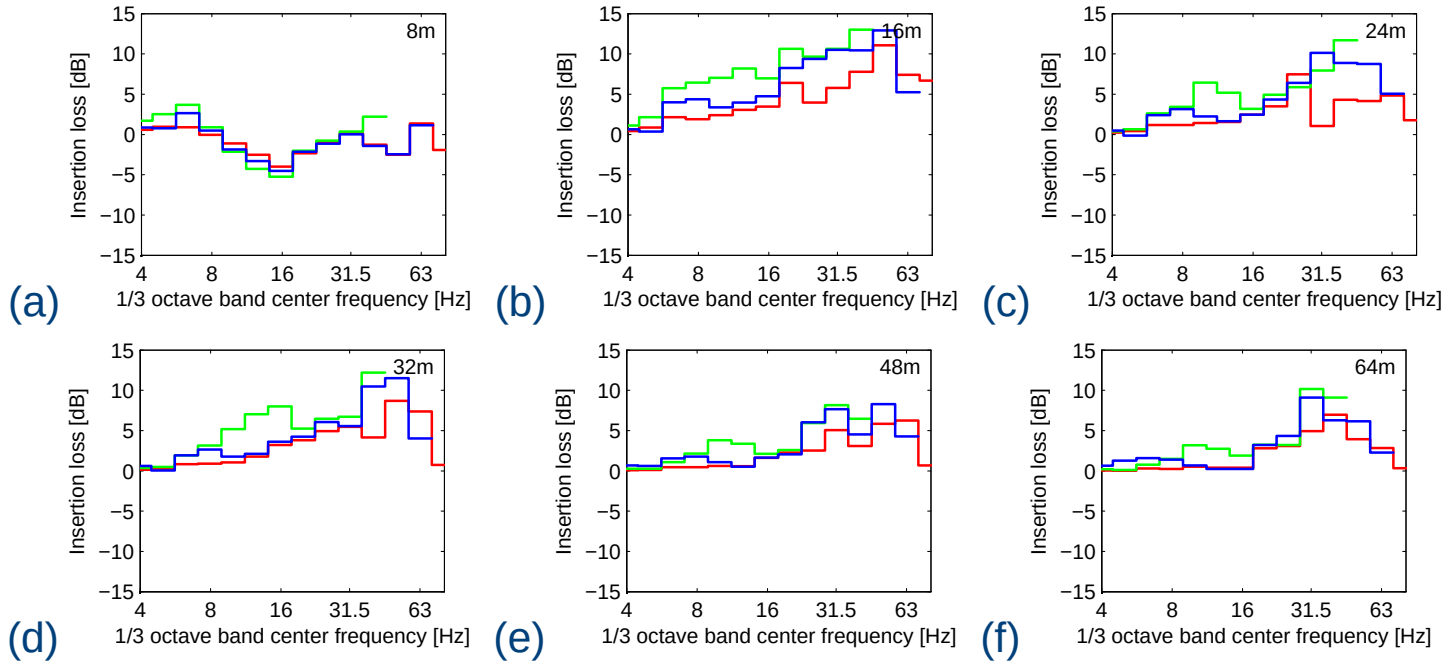

Column distribution

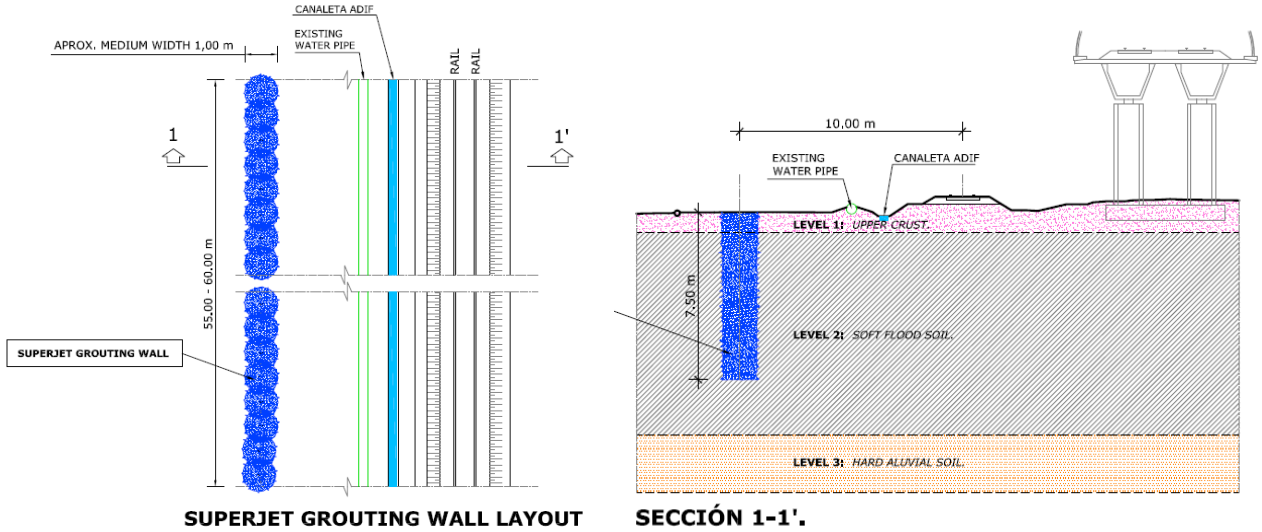

SUPERJET GROUTING WALL LAYOUT

SECCIÓN 1-1'.

Jet grouting method

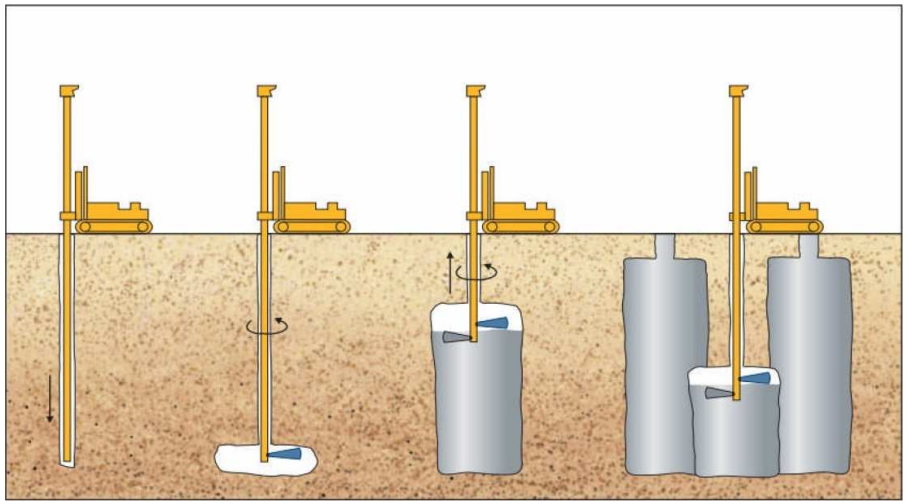

Installation

Conclusion

- Block of stiffened soil can behave as a wave impeding barrier.
- The wave impeding effect critically depends on the relation between λ_{R} and λ_{b}:
  - A reduction of vibration levels is only possible above a critical frequency f_{c} (if $\lambda_{\mathrm{b}} > \lambda_{\mathrm{R}}$).
  - Area of significant reduction is delimited by $\theta_{\mathrm{c}}(\omega) = \sin^{-1}\left(\lambda_{\mathrm{R}}/\lambda_{\mathrm{b}}\right)$
    $\Rightarrow$ expressions for f_{c} and $\theta_{\mathrm{c}}(\omega)$ are very useful in an early design stage.
- A stiff wave barrier is well suited at a site with soft soil layers.
- Jet grouting wall should be as stiff, deep, heavy and long as possible.
- Train passage: insertion loss $\widehat{\mathrm{IL}}_z(\mathbf{x}, \omega)$ is larger closer to the track and at higher frequencies.
- Numerical predictions indicate that subgrade stiffening at the test site in El Realengo can be very effective; a jet grouting wall is under construction and its vibration reduction efficiency will be assessed in an extensive measurement campaign.